Earthquake Engineering, Tenth World Conference © 1992 Balkema, Rotterdam. ISBN 90 5410 060 5

New method for time-domain analysis of dam-reservoir interaction

B.Weber
Swiss Federal Institute of Technology (ETH), Zurich, Switzerland

ABSTRACT: When analyzing the nonlinear earthquake behaviour of a dam one has to work in the time domain. On the other hand, the farfield solution of a reservoir with compressible water and the proper radiation boundary condition can only be formulated in the frequency domain. Usual procedures for the time domain, such as added mass or viscous boundaries, are inaccurate. Exact solutions using convolution are computationally inefficient.

In this paper we present a new method for the dam-reservoir interaction which includes compressibility of the water and a rigorous radiation boundary. The model works in the time domain and is obtained by an approximation of the frequency-domain solution. It is both accurate and efficient which is shown by several examples. Because the approximation has the same form as the finite element equations, the method is elegantly incorporated in a finite element program.

1 INTRODUCTION

Much progress has been made in the past towards more realistic earthquake analysis of concrete gravity and arch dams. Chopra and his coworkers (Chopra 1980, Fok 1985) have developed a theory and computer programs for the dam-reservoir interaction including compressibility of the water and the proper radiation boundary condition. Other researchers have worked on the nonlinear behaviour of dams, such as cracking of concrete and opening of joints (Dowling 1989, Hohberg 1992).

Dam-reservoir interaction with compressible water has to be solved in the frequency domain and is therefore only applicable to linear problems. Nonlinear behaviour of the dam, on the other hand, has to be solved in the time domain and the influence of the reservoir is usually included by crude simplifications such as the incompressible (added mass) model or viscous boundaries (Kausel 1988). Rigorous methods using convolution are computationally inefficient and need a large memory.

In this paper we present a new method for the dam-reservoir interaction which includes compressibility of the water and a rigorous radiation boundary but does not have the drawbacks of the commonly used procedures.

A typical model is shown in Figure 1. The three main parts of the model are the concrete dam with nonlinear joints, the irregular nearfield of the reservoir and an infinite channel for the farfield.

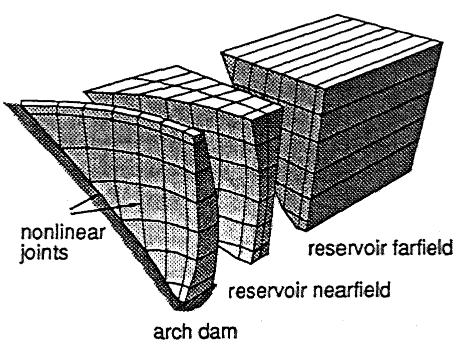

Figure 1: Dam-reservoir model

2 FINITE ELEMENT FORMULATION FOR THE NEARFIELD

The dam and the nearfield of the reservoir are modelled by standard finite elements. The dam is described by an isotropic linear elastic continuum. The fluid is assumed to be compressible, irrotational with small velocity amplitudes and is governed by the wave equation for the velocity potential φ as

$$c^2\Delta\varphi = \ddot{\varphi} \tag{1}$$

where c denotes the wave velocity of fluid. An absorptive foundation is introduced through the boundary condition

$$\frac{\partial \varphi}{\partial n} + q\dot{\varphi} = \bar{v}_n \tag{2}$$

where q is a parameter determining the amount of energy absorption and $\bar{v}_n$ is the prescribed normal velocity at the reservoir bottom. For the finite element formulation of the solid and the fluid we follow Bathe (1985). For the coupling between the solid and the fluid, interface elements are employed that have displacements and velocity potential as degrees of freedom. The system of equations for the coupled model is symmetric.

In the following we only look at the fluid equations. To later include the farfield (infinte channel), the fluid matrices are partitioned into the degrees of freedom of the interior of the nearfield (subscript 1) and the ones at the interface between the nearfield and the farfield (subscript 2).

$$\begin{bmatrix} \mathbf{S}_{11} & \mathbf{S}_{12} \\ \mathbf{S}_{21} & \mathbf{S}_{22} \end{bmatrix} \begin{bmatrix} \varphi_1 \\ \varphi_2 \end{bmatrix} = \begin{bmatrix} \mathbf{v}_1 \\ \mathbf{v}_2 \end{bmatrix} \tag{3}$$

The above equation is a compact form for the finite element formulation with $\mathbf{S}_{ij} = s^2\mathbf{M}_{ij} + s\mathbf{C}_{ij} + \mathbf{K}_{ij}$ for $i, j = 1, 2$. Although the equations are formally written in the Laplace domain, Equation (3) should be viewed as shorthand for the time domain equations. To simplify notation the same symbols are used for variables in the time domain and in the frequency domain. The nodal velocities $\mathbf{v}_1$ and $\mathbf{v}_2$ describe the input to the fluid system, analogously to the forces for the solid system. Specifically $\mathbf{v}_2$ describes the influence of the farfield to the nearfiled of the fluid.

3 FARFIELD SOLUTION IN THE FREQUENCY DOMAIN

The farfield solution of the fluid is first considered in the frequency domain. Separation of variables and discretizing the cross-section of the infinite channel by finite elements yields for the nodal velocity potential $\mathbf{\Phi}$ of the cross-section

$$(\mathbf{K}_I + i\omega\mathbf{C}_I - \omega^2\mathbf{M}_I)\mathbf{\Phi} = -k^2\mathbf{A}_I\mathbf{\Phi} + \mathbf{V}_I \tag{4}$$

The damping matrix $\mathbf{C}_I$ includes the reservoir bottom absorption. k is the wave number. The matrix $\mathbf{A}_I$ is a weighting matrix and is, for a constant wave velocity, $\mathbf{A}_I = c^2\mathbf{M}_I$. The velocity term $\mathbf{V}_I$ comes in through the boundary integrals of the variational form and represents the velocity boundary condition at the interface between the infinite channel and the foundation.

The total solution $\mathbf{\Phi}$ is obtained by superposition of the response $\mathbf{\Phi}^h$ due to an excitation normal to the cross-section of the channel and the response $\mathbf{\Phi}^p$ due to an excitation in the plane of the cross-section.

$$\mathbf{\Phi} = \mathbf{\Phi}^h + \mathbf{\Phi}^p \tag{5}$$

For an upstream excitation, there is no velocity input, i.e. $\mathbf{V}_I = 0$ and Equation (4) is an eigenvalue problem

$$(\mathbf{K}_I + i\omega\mathbf{C}_I - \omega^2\mathbf{M}_I)\mathbf{\Psi} = \mathbf{A}_I\mathbf{\Psi}\mathbf{k}^2 \tag{6}$$

where now $\mathbf{\Psi}$ has been used to denote the matrix of eigenvectors. They are orthogonal and normalized to $\mathbf{\Psi}\mathbf{A}_I\mathbf{\Psi}^T = \mathbf{I}$. The matrix $\mathbf{k} = \mathbf{diag}(ik_1, \ldots, ik_n)$ containes the stiffness of each mode. The sign has to be chosen to satisfy the radiation condition, i.e. $\pi < \arg k \leq 2\pi$. Expressing the nodal velocity potential as $\mathbf{\Phi}^h = \mathbf{\Psi}\boldsymbol{\eta}$ yields for the velocity

$$\mathbf{v}_2 = -\mathbf{A}_I\mathbf{\Psi}\mathbf{k}\boldsymbol{\eta} = -\mathbf{A}_I\mathbf{\Psi}\mathbf{k}\mathbf{\Psi}^T\mathbf{A}_I\mathbf{\Phi}^h \tag{7}$$

For the vertical or the cross-stream direction, the excitation is assumed to be uniform along the channel, i.e. independent of x. Then $k_i = 0$ and Equation (4) reduces to

$$(\mathbf{K}_I + i\omega\mathbf{C}_I - \omega^2\mathbf{M}_I)\mathbf{\Phi}^p = \mathbf{V}_I \tag{8}$$

This problem is solved directly in the time domain. With the nodal velocity potential $\varphi_2 = \mathbf{\Phi}$ and considering Equations (5) and (7), the final relationship is

$$\mathbf{v}_2 = -\mathbf{A}_I\mathbf{\Psi}\mathbf{k}\mathbf{\Psi}^T\mathbf{A}_I(\mathbf{\Phi} - \mathbf{\Phi}^p) = -\mathbf{G}(s)(\varphi_2 - \mathbf{\Phi}^p) \tag{9}$$

Sofar the method is standard and has been widely used for frequency-domain analysis of infinite domains (Fok 1985).

The $N \times N$ matrix $\mathbf{G}(s)$ is frequency dependent. The classical method to transform it to the time domain is to employ the Fourier transform. This leads to the impulse function $\mathbf{g}(t)$ which in this case consists of an $N \times N$ matrix for each of the N_T time steps. This means that $N_T N^2$ items have to stored. Typical values for a dam-reservoir-interaction problem are $N = 100$ and $N_T = 1000$, leading to an impuls respose matrix of 10^7 entries. The number of multiplications to perform the convolution is $N^2 N_T^2/2$, typically $5 \cdot 10^9$. The large number of entries to be stored and of operations to be performed makes it necessary to find a method that reduces the computational effort drastically.

A first step in reducing the computational effort of evaluating Equation (9) in the time domain is to make use of the modal decomposition of the problem. If the bottom absorption is neglected and in addition the wave velocity is the same for all elements then $\mathbf{C}_I = 0$ and $\mathbf{A}_I = c^2\mathbf{M}_I$. In this case Equation (6) reduces to

$$\mathbf{K}_I = \mathbf{A}_I\mathbf{\Psi}_0\mathbf{\Lambda}^2 \tag{10}$$

with $\mathbf{\Lambda}^2 = \mathbf{k}^2 + \omega^2/c^2\mathbf{I}$. In this case the eigenvectors are frequency independent. Each mode can therefore be treated separately, reducing the impuls matrix to $N \times N_T$ (typically 10^4) entries or even less if only a few modes are considered. This idea has been followed by Tsai (1987).

Another idea to reduce the computational effort is to use a subspace solution (Ritz vectors). We assume that the frequency-dependent eigenvectors Ψ may be expressed by the frequency-independent (basis) vectors Ψ_0 as

$$\Psi = \Psi_0 \Psi^* \tag{11}$$

where the matrices Ψ and Ψ_0 are $N \times N_\psi$ but the matrix Ψ^* is only $N_\psi \times N_\psi$ with N_ψ the number of modes considered. The basis Ψ_0 is taken to be the eigenvectors for $\omega = 0$. The eigenvalue problem Equation (6) is reformulated as

$$(\mathbf{K}_I^* + i\omega \mathbf{C}_I^* - \omega^2 \mathbf{M}_I^*)\Psi^* = \Psi^* \mathbf{k}^2 \tag{12}$$

with $\mathbf{K}_I^* = \Psi_0^T \mathbf{K}_I \Psi_0$, $\mathbf{C}_I^* = \Psi_0^T \mathbf{C}_I \Psi_0$ and $\mathbf{M}_I^* = \Psi_0^T \mathbf{M}_I \Psi_0$. The eigenvalue problem is thus reduced to $N_\psi \times N_\psi$ and has standard form. Only for $\omega = 0$ the full $N \times N$ generalized eigenvalue problem (Equation 6) has to be solved. The stiffness of the infinite domain is then

$$\mathbf{G}(s) = \mathbf{A}_I \Psi_0 \mathbf{k}^* \Psi_0^T \mathbf{A}_I \tag{13}$$

with $\mathbf{k}^* = \Psi^* \mathbf{k} \Psi^{*T}$. Except for the case where the eigenvectors are frequency independent, $\mathbf{k}^*(s)$ is a full matrix but much smaller than the original matrix $\mathbf{G}(s)$. The impuls matrix for the subspace problem is $N_T \times N_\psi \times N_\psi$, typically 10^5 for $N_\psi = 10$. If the bottom absorption is only small, the off-diagonal terms of $\mathbf{k}^*$ can be neglected as an approximation.

4 TIME DOMAIN APPROXIMATION

To really cut down on the computational effort, a new method is introduced. The frequency-dependent stiffness $\mathbf{k}^*$ is approximated by a linear time-invariant system. This system is first written in the standard form of linear system theory as

$$\mathbf{F}(s) = \mathbf{k}^* - \mathbf{D}_1 s = \mathbf{C}(\mathbf{I}s - \mathbf{A})^{-1}\mathbf{B} + \mathbf{D} \tag{14}$$

The term $\mathbf{D}_1 s = i\omega/c\mathbf{I}$ has to be subtracted in order to get a system with a regular high-frequency behaviour (a proper system) and can be added later simply as a dashpot. The formulation is very general and allows to take advantage of many results of linear system theory. After the approximation, the results will be recast into the standard form of the finite element formulation. Only a small number of additional internal degrees of freedom result which are appended to the finite element system of the nearfield.

The method consists of a number of steps which are outlined in the following. Some more explanations are given in Weber (1990) where the major steps are illustrated for a scalar example.

4.1 Bilinear Transformation

The method makes use of the Hankel matrix of the system. As it is much easier to find the Hankel matrix of a discrete-time system than that of a continuous-time system, Equation (14) is first transformed to the discrete-time system

$$\tilde{\mathbf{F}}(z) = \tilde{\mathbf{C}}(\mathbf{I}z - \tilde{\mathbf{A}})^{-1}\tilde{\mathbf{B}} + \tilde{\mathbf{D}} \tag{15}$$

The approximation for the discrete-time system is later transformed back to the contiuous-time case.

The transformation from the continuous-time to the discrete-time case and back is done by the bilinear transformation

$$s = \alpha\frac{z-1}{z+1}; \qquad z = \frac{\alpha + s}{\alpha - s} \tag{16}$$

where $s = i\omega$ and $z = e^{i\Omega}$. ω and Ω are the frequencies of the continuous-time and the discrete-time system, respectively, and α is an arbitrary stretching parameter. They are related by

$$\omega = \alpha \tan \Omega/2 \tag{17}$$

The imaginary axis and the left half-plane of the s-plane (continuous time) are transformed to the unit circle and the unit disc of the z-plane (discrete time), respectively. The discrete-time transfer function on the unit circle is the same as the continuous-time transfer function on the imaginary axis except for a stretching according to Equation (17).

$$\mathbf{F}(i\alpha \tan \Omega/2) = \tilde{\mathbf{F}}(e^{i\Omega}) \tag{18}$$

A regular spacing of the discrete-time frequencies Ω as needed for the Fast Fourier Transform corresponds to a favorable spacing of the continuous-time frequencies ω: dense for lower frequencies, sparse for higher frequencies up to $\omega = \infty$ corresponding to $\Omega = \pi$.

4.2 Realization by Singular Value Decomposition

The following procedure for approximating the discrete-time system is described in Chen (1984). The first step consists of finding the Hankel matrix. For a discrete-time system, the entries of the Hankel matrix are the valus $\mathbf{f}_k$ of the impuls function, which may be found by the Fast Fourier Transform.

$$\mathbf{H} = \begin{bmatrix} \mathbf{f}_1 & \mathbf{f}_2 & \mathbf{f}_3 & \cdots \\ \mathbf{f}_2 & \mathbf{f}_3 & \mathbf{f}_4 & \cdots \\ \mathbf{f}_3 & \mathbf{f}_4 & \cdots & \cdots \\ \cdots & \cdots & \cdots & \cdots \end{bmatrix} \tag{19}$$

The Hankel matrix playes an important role in system theory. The rank of $\mathbf{H}$ is knwon to be equal to the minimal degree of the system (= dimension of $\tilde{\mathbf{A}}$). A numerically reliable procedure to find the rank of a matrix is the singular value decomposition (Golub 1986).

$$\mathbf{H} = \mathbf{U}\boldsymbol{\Sigma}\mathbf{V}^T = \begin{bmatrix} \mathbf{U}_1 & \mathbf{U}_2 \end{bmatrix} \begin{bmatrix} \boldsymbol{\Sigma}_1 & \\ & \boldsymbol{\Sigma}_2 \end{bmatrix} \begin{bmatrix} \mathbf{V}_1^T \\ \mathbf{V}_2^T \end{bmatrix} \quad (20)$$

$\mathbf{U}$ and $\mathbf{V}$ are unitary matrices and $\boldsymbol{\Sigma}$ is a diagonal matrix containing the singluar values $\sigma_1 \geq \sigma_2 \geq \cdots \geq \sigma_r \geq \sigma_{r+1} \geq \cdots \geq 0$. The (numerical) rank r of $\mathbf{H}$ is determined such that the $\sigma_{r+1} \geq \cdots \geq 0$ are negligable. In practical examples the singular values decrease rapidely and r is a small number. The partitioning in Equation (20) is done such that $\boldsymbol{\Sigma}_1 = \mathbf{diag}(\sigma_1, \ldots, \sigma_r)$ containes the nonnegligable and $\boldsymbol{\Sigma}_2$ the negligable singular values. The Hankel matrix is therefore

$$\mathbf{H} = \mathbf{U}_1\boldsymbol{\Sigma}_1\mathbf{V}_1^T \quad (21)$$

For the discrete-time system $(\tilde{\mathbf{A}}, \tilde{\mathbf{B}}, \tilde{\mathbf{B}}, \tilde{\mathbf{D}})$, the impuls function is

$$\begin{aligned} \mathbf{f}_0 &= \tilde{\mathbf{D}} & (22) \\ \mathbf{f}_k &= \tilde{\mathbf{C}}\tilde{\mathbf{A}}^{k-1}\tilde{\mathbf{B}} \quad k \geq 1 & (23) \end{aligned}$$

so the Hankel matrix may be expressed as the product of the observability matrix $\mathbf{W}_o$ and the controllability matrix $\mathbf{W}_c$ as follows:

$$\mathbf{H} = \mathbf{W}_o\mathbf{W}_c = \begin{bmatrix} \mathbf{C} \\ \mathbf{CA} \\ \mathbf{CA}^2 \\ \vdots \end{bmatrix} \begin{bmatrix} \mathbf{B} & \mathbf{AB} & \mathbf{A}^2\mathbf{B} & \cdots \end{bmatrix} \quad (24)$$

Comparing this equation to Equation (21) one can see that the observability and the controllability matrices are given by

$$\mathbf{W}_o = \mathbf{U}_1\boldsymbol{\Sigma}_1^{1/2}\ ; \ \ \mathbf{W}_c = \boldsymbol{\Sigma}_1^{1/2}\mathbf{V}_1^T \quad (25)$$

Due to the fact that $\mathbf{U}$ and $\mathbf{V}$ are unitary, the pseudo-inverses are easily found to be

$$\mathbf{W}_o^+ = \boldsymbol{\Sigma}_1^{-1/2}\mathbf{U}_1^T\ ; \ \ \mathbf{W}_c^+ = \mathbf{V}_1\boldsymbol{\Sigma}_1^{-1/2} \quad (26)$$

We further need to form the shifted Hankel matrix

$$\widehat{\mathbf{H}} = \begin{bmatrix} \mathbf{f}_2 & \mathbf{f}_3 & \cdots \\ \mathbf{f}_3 & \mathbf{f}_4 & \cdots \\ \cdots & \cdots & \cdots \end{bmatrix} = \mathbf{W}_o\tilde{\mathbf{A}}\mathbf{W}_c \quad (27)$$

from which the matrix $\tilde{\mathbf{A}}$ can be calculated as

$$\tilde{\mathbf{A}} = \mathbf{W}_o^+\widehat{\mathbf{H}}\mathbf{W}_c^+ \quad (28)$$

The matrices $\tilde{\mathbf{B}}$ and $\tilde{\mathbf{C}}$ are found by extracting the submatrices from $\mathbf{W}_c$ and $\mathbf{W}_o$ respectively, according to Equation (24). The matrix $\tilde{\mathbf{D}}$ finally is equal to $\mathbf{f}_0$. The above procedure works equally well for single-input, single-output systems as for multi-input, multi-output systems.

The discrete-time system $(\tilde{\mathbf{A}}, \tilde{\mathbf{B}}, \tilde{\mathbf{B}}, \tilde{\mathbf{D}})$ may now be transformed back to a continuous-time system (Glover 1984).

$$\begin{aligned} \mathbf{A} &= \alpha(\mathbf{I} + \tilde{\mathbf{A}})^{-1}(\tilde{\mathbf{A}} - \mathbf{I}) & (29) \\ \mathbf{B} &= \sqrt{2\alpha}\,(\mathbf{I} + \tilde{\mathbf{A}})^{-1}\tilde{\mathbf{B}} & (30) \\ \mathbf{C} &= \sqrt{2\alpha}\,\tilde{\mathbf{C}}(\mathbf{I} + \tilde{\mathbf{A}})^{-1} & (31) \\ \mathbf{D} &= \tilde{\mathbf{D}} - \tilde{\mathbf{C}}(\mathbf{I} + \tilde{\mathbf{A}})^{-1}\tilde{\mathbf{B}} & (32) \end{aligned}$$

4.3 Second-order Symmetric System

It remains to transform the first-order system to a second-order symmetric system. Although this is not an essential step, it is convenient to have the system obtained from the farfield approximation in the same form as the finite element matrices.

By solving an eigenvalue problem, the matrix $\mathbf{A}$ can be diagonalized (to be assumed) and, by properly scaling the transformation matrix, the first-order system can be transformed to

$$\mathbf{F}(s) = \hat{\mathbf{B}}^T(s\mathbf{I} - \boldsymbol{\Lambda})^{-1}\hat{\mathbf{B}} + \mathbf{D} \quad (33)$$

This symmetric form is always possilble because the system is input-output symmetric. Since the original matrix $\mathbf{A}$ is real, the corresponding rows of $\hat{\mathbf{B}}$ are either real or they appear as complex conjugate pairs. In partitioned form with index r for the real values and index c for the complex values we write

$$\begin{aligned} \mathbf{F}(s) = {} & \mathbf{B}_r^T(s\mathbf{I} - \boldsymbol{\Lambda}_r)^{-1}\mathbf{B}_r \\ & + \mathbf{B}_c^T(s\mathbf{I} - \boldsymbol{\Lambda}_c)^{-1}\mathbf{B}_c + \bar{\mathbf{B}}_c^T(s\mathbf{I} - \bar{\boldsymbol{\Lambda}}_c)^{-1}\bar{\mathbf{B}}_c + \mathbf{D} \quad (34) \end{aligned}$$

This equation has to be transformed to a second-order symmetric system of the general form

$$\begin{aligned} \mathbf{F}(s) = {} & (\mathbf{B}_1 s + \mathbf{B}_2)^T(\mathbf{A}_0 s^2 + \mathbf{A}_1 s + \mathbf{A}_2)^{-1}(\mathbf{B}_1 s + \mathbf{B}_2) \\ & + \mathbf{D}_2 \quad (35) \end{aligned}$$

The terms corresponding to real eigenvalues are already in this form. They correspond to a system with stiffness and damping but no mass. However, to not preclude explicit time integration, the form with damping and mass but no stiffness is prefered.

$$\begin{aligned} & \mathbf{A}_0 = -\mathbf{I}\ ; \ \ \mathbf{A}_1 = \boldsymbol{\Lambda}_r\ ; \ \ \mathbf{A}_2 = \mathbf{0} & (36) \\ & \mathbf{B}_1 = (-\boldsymbol{\Lambda}_r)^{-1/2}\mathbf{B}_r\ ; \ \ \mathbf{B}_2 = \mathbf{0} & (37) \\ & \mathbf{D}_2 = \mathbf{D} - \mathbf{B}_1^T\mathbf{B}_1 & (38) \end{aligned}$$

The minus sign in $(-\boldsymbol{\Lambda}_r)^{-1/2}$ is necessary because for a stable system the eigenvalues are negative. The additional constant term in $\mathbf{D}_2$ accounts for the high-frequency behaviour.

Each pair of complex conjugate eigenvalues forms a second-order system. With $\mathbf{E} = (\boldsymbol{\Lambda}_c - \bar{\boldsymbol{\Lambda}}_c)^{-1/2}\mathbf{B}_c$ the second-order matrices are

$$\begin{aligned} & \mathbf{A}_0 = \mathbf{I}\ ; \ \ \mathbf{A}_1 = \boldsymbol{\Lambda}_c + \bar{\boldsymbol{\Lambda}}_c\ ; \ \ \mathbf{A}_2 = \boldsymbol{\Lambda}_c\bar{\boldsymbol{\Lambda}}_c & (39) \\ & \mathbf{B}_1 = \mathbf{E} + \bar{\mathbf{E}}\ ; \ \ \mathbf{B}_2 = \mathbf{E}\bar{\boldsymbol{\Lambda}}_c + \bar{\mathbf{E}}\boldsymbol{\Lambda}_c & (40) \\ & \mathbf{D}_2 = \mathbf{D} - \mathbf{B}_1^T\mathbf{B}_1 & (41) \end{aligned}$$

All system matrices are real because they consist of sums or products of complex conjugate pairs. The additional constant term in $\mathbf{D}_2$ accounts for the high frequency-behaviour.

4.4 Stability and Causality

Important points of the approximation are stability and causality. A system is stable if, for a bounded input, the output is also bounded. For a discrete-time system this means that all poles (eigenvalues of $\tilde{\mathbf{A}}$) must have an absolute value of less than one, for a continuous-time system the poles must have a negative real part. A system is causal if its impuls response is zero for negative times, meaning that the present does not affect the past. For finite-dimensional time-invariant systems (as is the approximation) the condition of zero impulse response for negative times is equivalent to the stability condition for the poles. If the original system is causal, it can be expected that the approximation is also causal and hence stable. However, small errors in the approximation may introduce anti-causal (and hence unstable) poles. They can be removed by neglecting the corresponding terms in Equation (33). It can be shown by Parseval's theorem that this does not increase the approximation error in the Euclidean norm.

4.5 Coupling of Nearfield and Farfield Equations

Again for compactness of notation Equation (13) is written as

$$\mathbf{G}(s) = \mathbf{R}^{\mathrm{T}}\mathbf{S}^{-1}\mathbf{R} + \mathbf{Q} \tag{42}$$

with

$$\mathbf{R} = (\mathbf{B}_1 s + \mathbf{B}_2)\mathbf{\Psi}_0^{\mathrm{T}}\mathbf{A}_I \tag{43}$$
$$\mathbf{S} = \mathbf{A}_0 s^2 + \mathbf{A}_1 s + \mathbf{A}_2 \tag{44}$$
$$\mathbf{Q} = \mathbf{A}_I\mathbf{\Psi}_0(\mathbf{D}_1 s + \mathbf{D}_2)\mathbf{\Psi}_0^{\mathrm{T}}\mathbf{A}_I \tag{45}$$

The dashpot term $\mathbf{D}_1 s$ (see Equation 14) has been reintroduced. The relationship between the velocity and the velocity potential at the interface between the nearfield and the farfield is then (see Equation 9)

$$\mathbf{v}_2 = -\mathbf{R}^{\mathrm{T}}\mathbf{S}^{-1}\mathbf{R}(\varphi_2 - \mathbf{\Phi}^p) - \mathbf{Q}(\varphi_2 - \mathbf{\Phi}^p) \tag{46}$$

Introducing the variable $\boldsymbol{\xi} = \mathbf{S}^{-1}\mathbf{R}(\varphi_2 - \mathbf{\Phi}^p)$ we write

$$\mathbf{v}_2 = -\mathbf{R}^{\mathrm{T}}\boldsymbol{\xi} - \mathbf{Q}(\varphi_2 - \mathbf{\Phi}^p) \tag{47}$$

and the identity

$$\mathbf{S}\boldsymbol{\xi} = \mathbf{R}(\varphi_2 - \mathbf{\Phi}^p) \tag{48}$$

The matrix Equation (3) becomes

$$\begin{bmatrix} \mathbf{S}_{11} & \mathbf{S}_{12} & \\ \mathbf{S}_{21} & \mathbf{S}_{22}+\mathbf{Q} & \mathbf{R}^{\mathrm{T}} \\ & \mathbf{R} & -\mathbf{S} \end{bmatrix} \begin{bmatrix} \varphi_1 \\ \varphi_2 \\ \boldsymbol{\xi} \end{bmatrix} = \begin{bmatrix} \mathbf{v}_1 \\ \mathbf{Q}\mathbf{\Phi}^p \\ \mathbf{R}\mathbf{\Phi}^p \end{bmatrix} \tag{49}$$

This is the final form of the equations used in the time integration procedure. Keeping in mind that $\mathbf{R}, \mathbf{S}$ and $\mathbf{Q}$ are matrix polynomials in s of at most second degree, Equation (49) is seen to be of the form $\mathbf{M}s^2 + \mathbf{C}s + \mathbf{K}$ which is really a compact notation for a system of second-order differential equations. The subspace approximation was essential because the frequency independet $\mathbf{\Psi}_0$ appears now in the system instead if $\mathbf{\Psi}(s)$.

5 EXAMPLES

The new method described in this paper has been implemented in a computer program called DanaiD (Dynamic Analysis of Infinte Domains).

As a first example the three-dimensional problem of a reservoir with semi-circular cross-section of 100 m radius is considered. The finite element discretization is shown in Figure 2. A small absorption

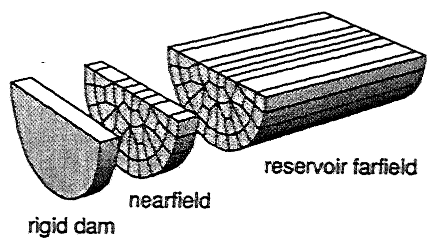

Figure 2: Semi-circular reservoir: Finite element discretization

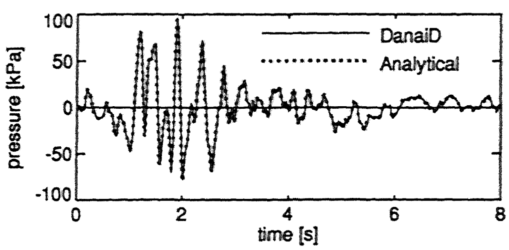

Figure 3: Semi-circular reservoir: Pressure due to horizontal (upstream) excitation

at the reservoir bottom ($q = 0.001$ s/m) is included. The dam is assumed to be rigid and subjected to an upstream earthquake excitation with a peak ground acceleation of 0.1 g. The subspace solution is taken with 10 modes. For the approximation only the diagonal terms of $\mathbf{k}^*$ are considered, leading to 23 internal degrees of freedom for the farfield. Figure 3 shows the pressure time history at 60 m depth. The results match the analytical values (Szczesiak and Weber 1992) perfectly.

The second example shows the same model subjected to a vertical ground motion of 2/3 of the horizontal one. Because a rigid dam is assumed, only the two-dimensional problem of the cross-section for Φ^p has to be solved. As seen in Figure 4 the match of the approximation and the analytical solution is again perfect.

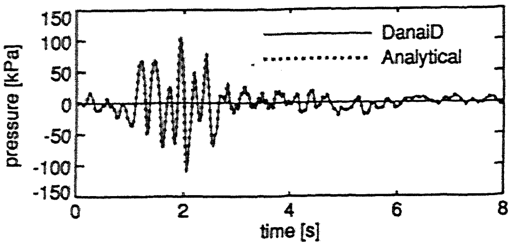

Figure 4: Semi-circular reservoir: Pressure due to vertical excitation

The third example shows an interaction problem with a flexible dam. The example is the Pine Flat dam subjected to the Taft earthquake as described in Chopra (1980). Figure 5 shows the finite element model. The dam consists of 136 4-node solid elements. The reservoir nearfield is modelled by one column of 16 fluid elements. The subspace solution with 5 modes and diagonal approximation leads to 10 internal degrees of freedom, a small number compared to the 338 degrees of freedom for the reservoir nearfiled and the dam.

In Figure 6, the horizontal displacement of the dam crest computed by the new method is compared to the results given in the reference (EAGD).

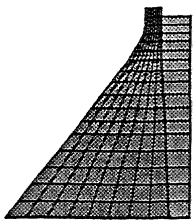

Figure 5: Pine Flat: Finite element mesh

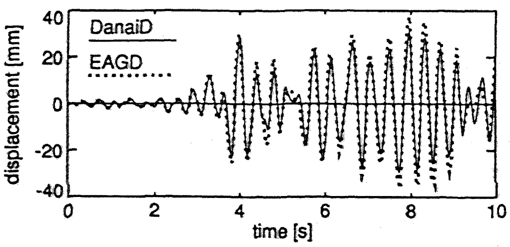

Figure 6: Pine Flat: Horizontal displacement of dam crest

6 CONCLUSIONS

A new method for treating a reservoir with compressible water and a rigorous radiation boundary condition in the time domain is presented. Contrary to standard methods such as added mass or viscous boundaries, the method is accurate and, contrary to (accurate) convolution methods, it is also efficient. The method is based on an approximation of the frequency-domain solution by a linear time-invariant system which has the same form as the finite element system. The method is thus suitable for an earthquake analysis of a complete dam-reserevoir model with nonlinear behaviour of the dam and the nearfield reservoir. Various examples show the applicability and effectiveness of the method to large dam-fluid models.

REFERENCES

Bathe, K.-J. & L.G. Olson 1985. Analysis of fluid-structure interactions. A direct symmetric coupled formulation based on the velocity potential. Comp. & Struct. 21: 21–32.

Chen, C.-T. 1984. Linear System Theory and Design. New York: Holt, Rinehart & Winston.

Chopra, A.K. & P. Chakrabarti & S. Gupta 1980. Earthquake respose of concrete gravity dams including hydrodynamic and foundation interaction effects. Report No. EERC-80/01, Earthq. Eng. Cent. Univ. of Calif., Berkeley.

Dowling, J. & J.F. Hall 1989. Nonlinear seismic analysis of arch dams. J. Eng. Mech., ASCE, 115(4):768–789.

Fok, K.-L. & A.K. Chopra 1985. Earthquake analysis and response of concrete arch dams. Report No. EERC-85/07, Earthq. Eng. Cent. Univ. of Calif., Berkeley.

Glover, K. 1984. All optimal Hankel-norm approximations of linear multivariate systems and their L^∞-error bounds. Int. J. Control 39: 1115–1193.

Golub, G.H. & C.F. Van Loan 1986. Matrix Computations. North Oxford Academic Publishers, London.

Hohberg, J.-M. 1992. A joint element for the nonlinear dynamic analysis of arch dams. Dissertation, Swiss Federal Institute of Technology, Zurich.

Kausel, E. 1988. Local transmitting boundaries. J. Eng. ASCE 114: 1011–1027.

Szczesiak, T. & B. Weber 1992. Hydrodynamic effects in a reservoir with semi-circular cross-section and absorptive bottom. To appear in Soil Dyn. and Earth. Eng.

Tsai, Ch.-S. & G.C. Lee 1987. Arch dam-fluid interactions: by FEM-BEM and substructure concepts. Int. J. Num. Meth. Eng. 24: 2367–2388

Weber, B. 1990. Fluid-structure interaction for arch dams. Proc. Europ. Conf. Struct. Dyn. EURODYN'90, Bochum: 851–858.